PIBB 生物化学与生物物理进展
Progress in Biochemistry and Biophysics
2013, 40(2): 147~158
www.pibb.ac.cn

ZNF403, a Novel Cell Cycle Regulator*

GUAN Rui[1,2,3], HOU De-Fu[1,2], RAO Xiang[2], GUAN Yong-Jun[2],
OUYANG Yong-Mei[2], YU Yan-Hui[2], Jim HU[3], CHEN Zhu-Chu[1,2]**

([1] *Key Laboratory of Cancer Proteomics of Chinese Ministry of Health, Xiangya Hospital, Central South University, Changsha* 410008, China;
[2] *Cancer Research Institute, Xiangya School of Medicine, Central South University, Changsha* 410008, China;
[3] *Physiology and Experimental Medicine Program, Hospital for Sick Children, Toronto, Ontario* M5G1X8, Canada)

Abstract ZNF403 and LCRG1 are two alternative splicing isoforms from human gene ZNF403. Previous study shows that LCRG1 displays tumor-suppressive properties in laryngeal carcinoma cell line Hep-2 cells. The aim of this study is to clarify the relationships between these two isoforms and further investigate the role of ZNF403 in tumor cells. Realtime PCR analysis was first applied to demonstrate the relative abundance of these two isoforms and showed that ZNF403 is the major transcription product. The function of ZNF403 in cell growth was next accessed by MTT assay and tumor growth in nude mice analysis, respectively. The results indicated that ZNF403 knockdown resulted in inhibition of cell growth in Hep-2 cell both *in vitro* and *in vivo*. Moreover, bioinformatics analysis, flow-cytometric analysis and PCR array analysis were performed to elucidate the mechanism under the role of ZNF403 in cell growth. Knockdown of ZNF403 significantly decreased the rate of DNA synthesis and mitosis. Additionally, a number of key cell-cycle regulating components such as MCM2, p21, ATM and MRE11A were identified to be mediated by ZNF403. Altogether, our findings suggest that ZNF403 is a novel cell cycle regulator, which may play an essential role in tumorigenesis.

Key words ZNF403, LCRG1, alternative splicing, cell cycle, AhR
DOI: 10.3724/SP.J.1206.2012.00119

Laryngeal carcinoma (LC) which accounts for 25% head and neck carcinoma and 1% of all cancers, is the leading head and neck carcinoma[1]. Prolonged use of tobacco and excessive alcohol consumption are clearly associated with an increased incidence in laryngeal cancer[2–4]. Genetic factors are also responsible for individual susceptibility LC. It has been reported that the abnormal expression of EGFR, p53, CCND1, RB and Galectin-3 are associated with the tumorigenesis of LC [5]. Therefore, identification of proto-oncogenes and tumour suppressor genes are critical for an understanding of the biological initiation and progression of laryngeal cancer[6].

ZNF403, also known as GGNBP2 (gametogenetin binding protein 2) and DIF3 (dioxin inducible factor 3), is located on 17q12～21.1, a region associated with cancers such as laryngeal cancer, breast cancer and prostate cancer [7–8]. In human, there are two known RNA transcripts produced from ZNF403. The full size ZNF403 transcript is translated into a protein of 696 amino acids, which is the focus of the current study. The short transcript, laryngeal carcinoma related gene 1 (LCRG1), which encodes a nuclear protein of 288 amino acids, was originally identified in human laryngeal carcinoma by mRNA differential display. Previous studies demonstrated that LCRG1 is significantly reduced in human laryngeal cell line Hep-2 and ～40% of primary laryngeal. Over-expression of exogenous LCRG1 leads to growth suppression of Hep-2 cells[9–10].

Studies also have shown that Ggnbp2, the mouse homolog of ZNF403, is implicated to be associated with meiotic event during spermatogenesis [11–12].

*This work was supported by grants from RG is an awardee of The Chinese Scholarship Council (CSC). This work was partially supported by grants from The Canadian Institutes of Health Research to JH, The National Basic Research Program of China (2011CB9107040) and The National Natural Science Foundation of China (30973289, 81272971).

**Corresponding author.
Tel: 86-731-84327608, E-mail: tcbl@xysm.net

Received: May 15, 2012 Accepted: September 29, 2012

However, the exact function of the full size human ZNF403 remains to be discovered.

To investigate the role of ZNF403, in the present study, we reported the expression pattern of ZNF403 and LCRG1 in various human cell lines and then analyze the function of ZNF403 in Hep-2 cells both *in vitro* and *in vivo*. Furthermore, bioinformatics analysis, flowcytometric analysis and PCR array demonstrated its role in cell cycle regulation. Altogether, our findings provide a new insight into the function of ZNF403 in regulating cell growth and cell-cycle progression, implying down-regulating ZNF403 function may provide a promising strategy for tumor suppression in cancer therapy.

1 Materials and methods

1.1 Cell cultures

Hep-2 and HEK293 cells were grown in EMEM (Invitrogen) supplemented with 10% fetal bovine serum (FBS) (Invitrogen). A549 and BEAS-2B cells were grown in DMEM (Invitrogen) supplemented with 10% fetal bovine serum (FBS) (Invitrogen). Jurkat cells were grown in RPMI 1640 medium (Invitrogen) supplemented with 10% fetal bovine serum (FBS) (Invitrogen). Cell cultures were incubated in a humidified atmosphere containing 5% CO_2 at 37℃.

1.2 Virus transduction

HD-Ad-shRNA-ZNF403 and HD-Ad-shRNA-control were designed and produced as described in[13]. Hep-2 cells were seeded at 50%～60% confluency one day before transduction. Each virus was added to cells at 50 MOI in EMEM without FBS for 2 h (5 ml medium for 100 mm plates, 1 ml medium for one well in 6-well plates). The medium was then supplemented with 10% FBS. Transduced cells were incubated in a humidified atmosphere containing 5% CO_2 at 37℃ until harvested.

1.3 MTT assay

Hep-2 cells were seeded onto 24 well plates. A cell viability assay was performed every 24 h using the 3-(4, 5-dimethylthiazol-2-yl)-2, 5-diphenyltetrazolium bromide (MTT) assay. The cells were washed with PBS and 0.5 g/L MTT in serum free medium was added to the culture and incubated at 37℃ for 3 h. Formazan extraction was performed with isopropanol and the quantitation colorimetrically was performed by a spectrophotometer at 570 nm with the correction of interference at 690 nm. For each group, three independent experiments were performed in triplicate.

1.4 Tumor xenograft growth in nude mice

All mice were handled according to the Guide for the Care and Use of Laboratory Animals. For inoculation into nude mice, Hep-2 cells transduced with virus for 24 h were washed with PBS, digested with trypsin, resuspended in EMEM and pooled. After centrifugation, cells were counted and resuspended in PBS at a concentration of 2×10^6 cells per 100 μl. Cells of 100 μl were injected subcutaneously into 6-week-old female athymi nude mice on the dorsal surface. Mice were checked every two days for the xenograft growth. Tumor volumes and body weights were monitored every 2 d over the course of growth. Tumor volumes were monitored by caliper measurement of the length and width and calculated using the formula: Tumor volume/cm^3 = $d^2 \times D/2$, where d is the shortest and D is the longest diameter, respectively. Mice were sacrificed after 21 days of treatments and tumors were removed and fixed in 10% neutral buffered formalin.

1.5 Flow cytometric analysis

BrdU flow cytometric analysis was performed using FITC BrdU flow kit (BD Bioscience) according to the manufacturer's protocol. In brief, cells were stained with FITC conjugated anti-BrdU antibodies and 7-Aminoactinomycin D (7-AAD) for cell cycle analysis. Samples were analyzed by LSR Ⅱ flow cytometer (BD Bioscience) and the distribution of each cell-cycle phase was determined using FlowJo software (Tree Star Inc). Three independent experiments were performed in triplicate.

1.6 Quantitative real-time PCR

Real-time PCR analysis was carried out using the ABI Prism 7500 Sequence Detection System (Applied Biosystems) according to the manufacturer's protocol. The primers were designed by Primer Express software (Applied Biosystems) and synthesized from Sigma. The primer sequences are as follows: ZNF403-u-F, 5′ AGCTTAGTTGAACTCCTTGATGAGTCT 3′; ZNF403-u-R, 5′ CGGTATTGTTCTCTATTGCTG-TAGAAA 3′; LCRG1-u-F, 5′ TCGCCAAAGTT-CTGTGAACACT 3′; LCRG1-u-R, 5′ TGGTTT-GAGGAGGAATTGAGAAA 3′; ZNF403-c-F, 5′ GC-AC AGCTAAAGCAGTTCATTCA 3′; ZNF403-c-R, 5′ GACAACCAACACATGGGACAAG 3′; GAPDH-Forward, 5′ GAAGGTGAAGGTCGGAGTC 3′; GAPDH-Reverse, 5′ GAAGATGGTGATGGGATT-TC 3′.

Cells were harvested and total RNA was isolated using RNAspin mini columns (GE Healthcare), DNase

digestion was performed on columns. cDNA was synthesized from 1 μg of total RNA of each sample using Superscript Ⅱ reverse transcriptase (Invitrogen) following the manufacturer's protocol. The relative mRNA expression levels of each gene were determined using relative quantitation analysis by the comparative *C*t method with the formula $2^{-\Delta\Delta Ct}$. GAPDH was used as an internal control for normalization. Three independent experiments were done in triplicate.

1.7 Human cell-cycle Profiler PCR array

Total RNA was isolated using RNAspin mini (GE Healthcare). RT2 First Strand Kit (SABiosciences, Frederick, MD, USA) was used to synthesize cDNAs. The human cell-cycle PCR array (SABiosciences) was performed according to the manufacturer's protocol. Data were analyzed by SABioscience's web-based PCR array analysis software using the comparative *C*t method. Housekeeping genes(B2 M, HPRT1, RPL13A, and GAPDH) were used together for normalization. Three independent experiments were carried out. The *P* values are calculated based on Student's *t* test.

1.8 Western blots

Cells were washed with PBS and lysed in RIPA lysis buffer containing an EDTA-free protease inhibitor solution(Roche) at 4℃ for 30 min. Cell lysate was centrifuged at 14 000 r/min for 20 min at 4℃. Protein concentration was measured by a bicinchoninic acid (BCA) assay kit (Pierce). Protein samples (20 μg each) were separated by 10% SDS-PAGE and transferred to nitrocellulose membrane. The blots were incubated with specific primary antibodies: anti-ZNF403 (Sigma), anti-MCM2 (Abcam), anti-p21 (Abcam), anti-MRE11A(Abcam), anti-ATM (Abcam), anti-β -actin (Sigma), followed by HRP-conjugated secondary antibodies, and detected by an enhanced chemiluminescent substrate (Perkin Elmer).

2 Results

2.1 Expression of ZNF403 isoforms in human cell lines

ZNF403 is highly conserved from drosophila to human. From the protein sequence alignment, it showed that the mouse and human ZNF403 share more than 98% identity(Table 1). However, the short isoform LCRG1 is only reported to be exist in human. To understand the relative expression level of ZNF403 and its short alternative transcript LCRG1, we performed real-time PCR to examine their expression in different cell lines. As shown in Figure 1a, 3 pairs of primers were designed to determine their relative expression level. Z-c recognizes a common sequence which both transcripts contain, while L-u and Z-u only recognizes a unique sequence existing in LCRG1 or ZNF403 cDNA. As shown in Figure 1b, the expression level of ZNF403 is significantly higher (>10 folds) than that of LCRG1 in Hep-2, A549, Jurkat, BEAS-2B, HEK293 cell lines. Although the level of ZNF403 varied in these cell lines, the expression pattern of these two alternative transcripts was similar. These data suggest that ZNF403 is the major transcript produced from ZNF403 gene.

Table 1 ZNF403 (gametogenetin-binding protein 2) is highly conserved during evolution

Protein ID	Protein Name	Species	*ID*/%[1)]	Length/aa
NP_079111.1	Gametogenetin-binding protein 2	*H. sapiens*	100.0	696
XP_001173657.1	Zinc finger protein 403 isoform 3	*P. troglodytes*	100.0	696
XP_001111173.2	Gametogenetin-binding protein 2 like	*M. mulatta*	99.6	527
XP_001503854.2	Gametogenetin binding protein 2	*E. caballus*	99.6	695
XP_869049.3	Zinc finger protein 403 isoform 2	*B. taurus*	99.6	695
XP_002719125.1	Zinc finger protein 403	*O. cuniculus*	99.5	622
NP_694784.2	Gametogenetin binding protein 2	*M. musculus*	98.6	697
NP_001073430.1	Gametogenetin binding protein 2	*D. rerio*	85.1	624
NP_001088126.1	Gametogenetin binding protein 2	*X. laevis*	74.9	653

[1)] *ID* denotes percentage of amino acid identities between human ZNF403 protein and its homologues from different species.

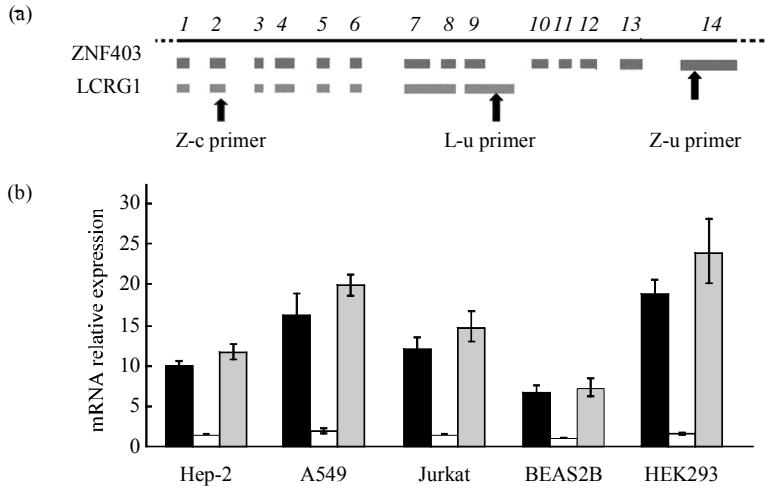

Fig. 1 Expression of ZNF403 and LCRG1 in different cell lines

(a) Comparison of mRNA structure between ZNF403 and LCRG1. Boxs represent exons of ZNF403 and LCRG1. Three pairs of primers were designed to detect the expression level of ZNF403 and LCRG1. Z-c recognizes a common sequence which both transcripts contain, while L-u and Z-u only recognizes a unique sequence existing only in LCRG1 or ZNF403 mRNA. (b) Realtime PCR analysis of mRNA expression of ZNF403 and LCRG1 in Hep-2, A549, Jurkat, BEAS-2B and HEK293 cells. ■: Z-u; □: L-u; ▨: Z-c.

2.2 Knockdown of ZNF403 reduced cell growth of tumor cells both *in vitro* and *in vivo*

Previous studies showed that the over expression of LCRG1, the shorter isoform, is associated with tumor suppression[9–10]. The pattern of expression level of ZNF403 and LCRG1 lead us to hypothesize that ZNF403 may be also involved in cell growth. In order to clarify this hypothesis, we next examined the impact of ZNF403 on cell proliferation. Helper-dependent adenoviral vector mediated ZNF403-RNAi system [13] which efficiently and specifically knockdown the expression of ZNF403 was used to down-regulate ZNF403. As shown in Figure 2a, the knockdown of ZNF403 was confirmed by both quantitative PCR and Western blot analysis compared to vector control group and shRNA-control group. MTT assay was then performed to access the impact of ZNF403 on cell proliferation *in vitro*. The results demonstrated that the cell growth of the ZNF403 knockdown group in Hep-2 cells was approximately 50% slower than the control groups from day 1 to day 4 before the cells were harvested (Figure 2b). These findings suggested that the deletion of ZNF403 reduced the cell growth rate, implying that ZNF403 may regulate cell proliferation positively.

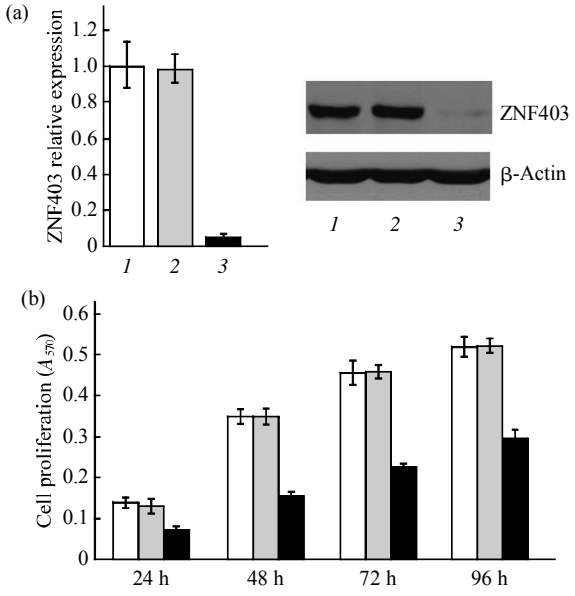

Fig. 2 Deletion of ZNF403 suppresses cell growth in Hep-2 cells

(a) Hep-2 cells were transduced by HD-Ad-ZNF403-shRNA (ZNF403-shRNA), HD-Ad-shRNA-control (shRNA-Ctrl), or the vector control for 24 h. Real-time PCR analysis was performed to assess the mRNA level of ZNF403. GAPDH was used as an internal control for normalization. Whole-cell lysates were analyzed by Western blotting to detect ZNF403 protein by rabbit anti-ZNF403 antibody. β-Actin served as a loading control. *1*: vec-Ctrl; *2*: shRNA-Ctrl; *3*: shRNA-ZNF403. (b) The cells transduced as decribed in (a) at indicated time point were washed with PBS and 0.5 g/L MTT in serum free medium was added to the culture and incubated at 37℃ for 3 h. Formazan extraction was performed with isopropanol and the quantitation colorimetrically was performed by a spectrophotometer. A representative result is shown from one of three independent experiments, each done in triplicate. Error bars indicate ± SE. * $P < 0.05$. □: vec-Ctrl; ▨: shRNA-Ctrl; ■: shRNA-ZNF403.

To validate our *in vitro* results, we performed xenograft experiments by treatment with helper dependent adenoviral vector in animal models. Hep-2 cells transduced with ZNF403-shRNA and shRNA-control were implanted subcutaneously in athymic mice. As shown in Figure 3, the knockdown of ZNF403 caused a ～50% reduction in tumor size as compared with the tumor volume of the control. We also calculated the growth delay as the number of days required to reach a tumor volume of 1000 mm^3 for treatment groups minus the number of days required for the control to reach the same volume, the knockdown of ZNF403 delayed tumor growth by approximately 7 and 10 days as compared with control.

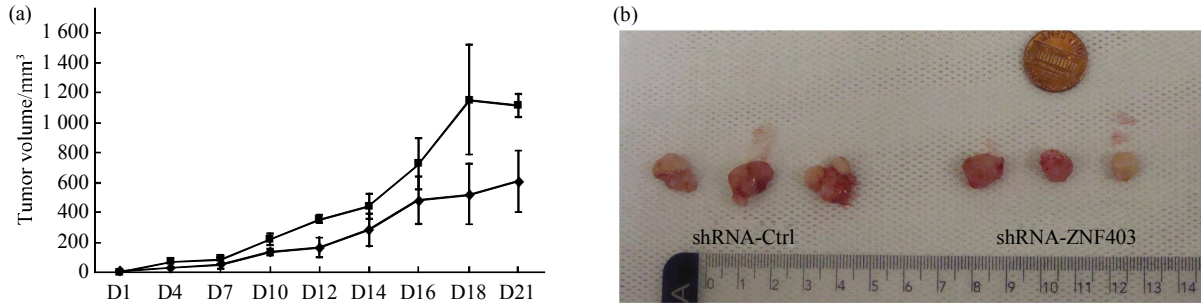

Fig. 3 Inhibition of tumor growth by ZNF403 knockdown in nude mice xenografted with human Hep-2 cells

(a) Tumor growth was recorded every 2 or 3 days by measuring its diameter with Vernier caliper. Tumor volume was calculated by tumor volume/cm^3 = $d^2 \times D/2$, where d is the shortest and D is the longest diameter, respectively. ♦—♦: ZNF403-shRNA; ■—■: shRNA-control. (b) Tumor volumes at sacrifice on day 21 were compared between mice treated with ZNF403-shRNA, shRNA-control. The pictures displayed representative tumors from each group.

2.3 Bioinformatics analysis of putative motifs

To elucidate the mechanism of ZNF403 in cell growth, we predicted putative motifs in ZNF403 by computation using the software Eukaryotic Linear Motif Resource for Functional site in Proteins [14]. A series of cell-cycle associated motifs, such as APC/C-binding Destruction motifs, cyclin-recognition sites, RB LXCXE binding motif, PCNA binding site, APCC binding destruction motif, and SCF-WD40 binding Phosphodegrons, were found in ZNF403 (Table 2). Interestingly, ZNF403 has a LKCDE motif (at amino acid positions 542～546), which is predicted

Table 2 Putative cell-cycle related motifs predicted in ZF403 by ELM software

Elm name	Matched sequence	Positions	Elm description	Motif pattern
LIG_APCC_Dbox_1	SREVLSALS	76～84	An RxxL-based motif that binds to the Cdh1 and Cdc20 components of APC/C thereby targeting the protein for destruction in a cell cycle dependent manner.	.R..L..[LIVM].
	KRCQLHSLD	160～168		
LIG_CYCLIN_1	KKLY	133～136	Substrate recognition site that interacts with cyclin and thereby increases phosphorylation by cyclin/cdk complexes. Predicted protein should have the MOD_CDK site. Also used by cyclin inhibitors.	[RK].L.{0,1}[FYLIVMP]
	KGLSP	455～459		
	KSLV	624～627		
LIG_PCNA	QDEIQSFMAN	645～654	The PCNA binding site is found in proteins involved in DNA replication, repair and cell cycle control.	((^.{0,3})|(Q)).[^FHWY][ILM][^P][^FHILVWYP][DHFM][FMY]..
LIG_Rb_LxCxE_1	LKCDE	542～546	Interacts with the Retinoblastoma protein.	[LI].C.[DE]
LIG_SCF_FBW7_1	IPTPLQT	389～395	The TPxxS phospho-dependent degron binds the FBW7 F box proteins of the SCF (Skp1_Cullin-Fbox) complex.	[LIVMP].{0,2}TP..[ST]
	PTPLQT	390～395		
LIG_USP7_1	ACGST	417～421	The USP7 NTD domain binding motif variant based on the MDM2 and P53 interactions.	PA][^P][^FYWIL]S[^P]
	PICSG	685～689		

to be a RB-binding LXCXE motif, a ligand to the conserved "pocket region" in the B-domain of the retinoblastoma proteins. RB LXCXE motif were found to exist in oncoproteins such as simian virus 40 T antigen, and human papillomavirus E7, as well as cellular proteins such as BRCA1, HDAC1 and HDAC2, which use it to interact with RB for regulating their functions. The cyclin recognition site, known as a Cy or RXL motif, was reported to bind directly to the cyclin subunit and exists in a wide range of cyclin/CDK interacting proteins such as the RB protein, p21. Proliferating cell nuclear antigen (PCNA), is a processivity factor of DNA polymerase, which encircles DNA during DNA replication and thus associates with the proliferative state of the cells. The PCNA binding site is found in proteins involved in DNA replication, DNA repair and cell cycle control. These bioinformatics' analysis results suggest that ZNF403 might be involved in cell-cycle progression and inspire us to investigate the role of ZNF403 in cell-cycle control.

2.4 Cell cycle analysis of ZNF403 using BrdU incorporation

To investigate the role of ZNF403 in cell cycle event, BrdU, which can be incorporated into DNA during S phase, was used to elucidate the role of ZNF403 in cell cycle in Hep-2 cells. ZNF403 knockdown and control cells were incubated with BrdU for different periods of time for up to 24 h. Flow cytometric analysis was then performed for the estimation of cell cycle phase distributions. As shown in Figure 4a, after incubation with BrdU for 2 h, the percentage of cells in S phase was reduced by ~10% and that of cells in G2/M phase was elevated by ~10% in the ZNF403 knockdown group compared to the control. To confirm observations above, we prolonged incubation of the transduced cells with BrdU for 4 h, consequently, the proportion of cells in S phase was also dropped down from ~40% to ~28% and the proportion of cells in G2/M phase was increased by ~10% in the ZNF403 knockdown group compared to the control (Figure 4b). Furthermore, we observed the cell distributions after incubation with BrdU for 24 h (Figure 4c). The results demonstrated that the percentage of Q1 cells (1N-DNA, BrdU+), which represents cells undergoing or have completed replication, was decreased by ~25% in the ZNF403 knockdown group. The percentage of Q2 cells (2N-DNA, BrdU+), a mixture of cells in late S phase and G2/M phase, was larger in the ZNF403knockdwon group than that of the control group by around ~25%. We also observed the percentage of Q3 cells (2N-DNA, BrdU-), which represents the cells that retained in G2/M phase prior to BrdU incubation, almost doubled in the ZNF403 knockdown group. Meanwhile, Q4 cells (1N-DNA, BrdU-), which are cells maintained in G1 phase, were approximately the same between the ZNF403-shRNA group and control group. Altogether, the cell cycle analysis indicated that

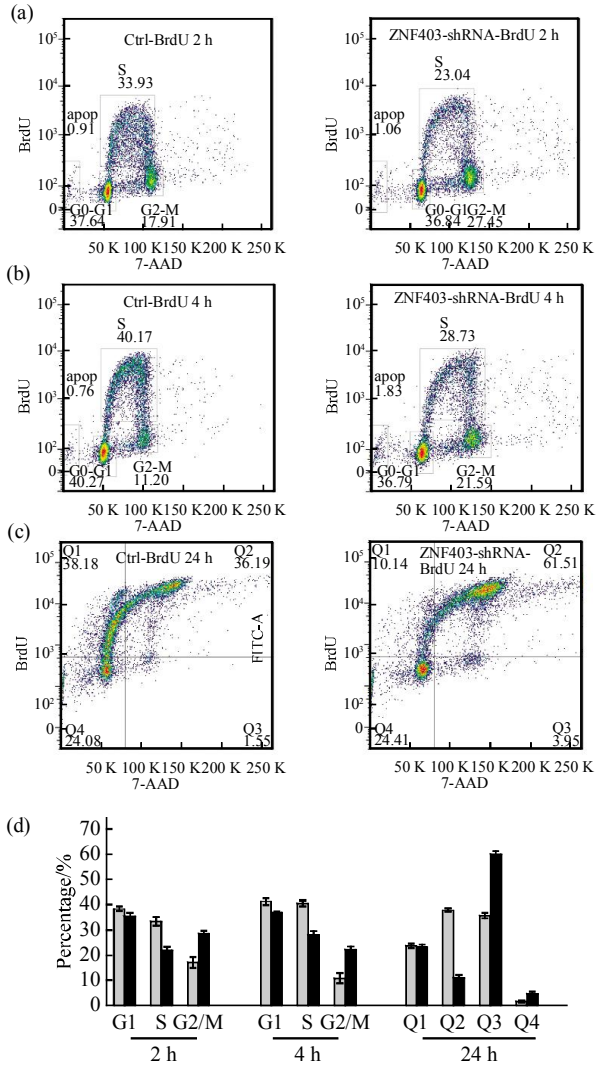

Fig. 4 Knockdown of ZNF403 decreased DNA synthesis and delayed mitosis

Hep-2 cells were transduced with control vector or ZNF403-shRNA at 50 MOI for 24 h and then labeled with BrdU for 2 h (a), 4 h (b) or 24 h (c). BrdU flow cytometric analysis was performed using FITC BrdU flow kit (BD Pharmingen) according to the manufacturer's protocol. In brief, cells were stained with FITC conjugated anti-BrdU antibodies and 7-Aminoactinomycin D (7-AAD) for cell cycle analysis. (d) The columns displayed the percentage of each cell-cycle phase. A representative result is shown from one of three independent experiments, each done in triplicate. □: shRNA-ctrl; ■: ZNF403-shRNA.

ZNF403 knockdown decreased the cells in S phase and accumulated in G2/M phase, which implying reduction of DNA synthesis and delay of mitosis.

2.5 Identification of down stream target genes regulated by ZNF403

To further reveal the mechanism of ZNF403 at molecular level in cell cycle networks, we carried out realtime PCR array in Hep-2 and HEK293 cells, respectively, to identify its down stream target genes. Cells were transduced with HD-Ad-shRNA-control or HD-Ad-shRNA-ZNF403, subsequently the ZNF403 knockdown cells and control cells were used to compare the expression level of cell cycle-genes by PCR array. As shown in the Figure 5a and 5b, the

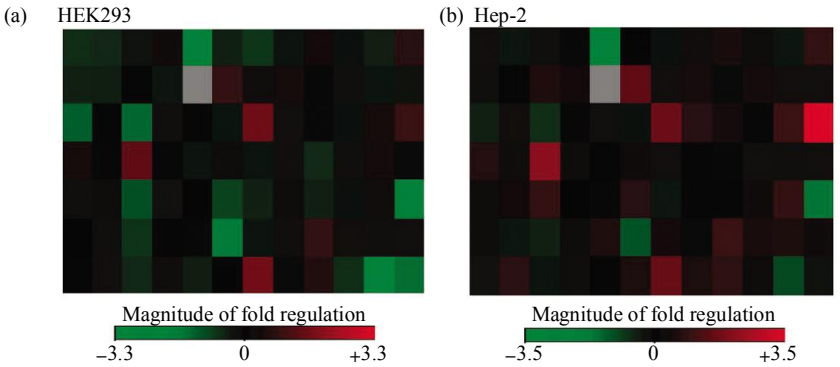

(c) Gene annotation

Catagory	Symbol	Description	Fold regulation		*P*-value
			In Hep-2	In HEK293	HEK293/Hep-2
Check points	ATM	Ataxia telangiectasia mutated	−2.7	−3.3	0.000159/0.000018
	CDKN1A	Cyclin dependent kinase inhibitor 1A (p21, Cip1)	3.5	1.6	0.000005/0.000082
	CDKN2B	Cyclin dependent kinase inhibitor 2B (p15, inhibits CDK4)	2.6	1.9	0.000139/0.000034
	TP53	Tumor protein p53	−1.8	−2.4	0.000122/0.00003
G1	SKP2	S-phase associated kinase protein 2(p45)	2.1	2.1	0.000034/0.000001
S	MCM2	Minichromosome maintenance complex component 2	−2.2	−2.9	0.000185/0.00001
G2	CDK5R1	Cyclin dependent kinase 5 regulatory subunit 1(p35)	2.2	2.1	0.003748/0.000014
M	MRE11A	MRE11 meiotic recombination 11 homolog A (*S. cerevisiae*)	−1.9	−2.2	0.00229/0.000122

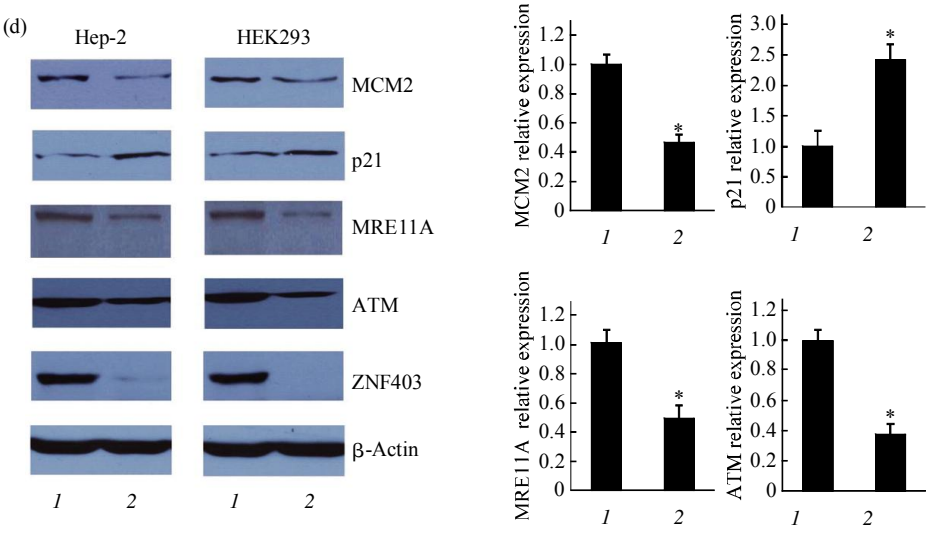

Fig. 5 Identification of ZNF403′s target genes by human cell-cycle PCR array analysis

HEK293 and Hep-2 cells were transduced with ZNF403-shRNA or shRNA-ctrl vector at 50 MOI. The Human Cell Cycle RT Profiler PCR Array (SABiosciences) was performed according to manufacturer's protocol. The heatmap displays the expression profile of 84 key cell-cycle genes in HEK293 (a) and Hep-2 (b) as a result of ZNF403 knockdown compared to control. Red represents increased expression while green indicates reduced expression. Data were analyzed by SABioscience's Web-based PCR array analysis software using the comparative *C*t method with the formula ($2^{-\Delta\Delta Ct}$). The *P*-values were calculated based on a Student's *t*-test of the triplicate samples. (c) Function annotations and expression details of significantly affected cell-cycle genes after ZNF403 knockdown. (d)The expression change of p21, MCM2, MRE11A and ATM in response to ZNF403 knockdown were confirmed by Western blot analysis. Each experiment was done in triplicate. Summary of mean band intensity of blot images was plotted on the right. Error bars indicate ± SE. * $P < 0.05$. *1*: shRNA-ctrl; *2*: ZNF403-shRNA.

heat-maps displayed the expression profile of 84 key cell-cycle genes in HEK293 and Hep-2 cells as a result of ZNF403 knockdown compared to control. Red represents increased expression while green indicates reduced expression. Moreover, the data analysis demonstrated that the mRNA levels of p21, skp2, CDK5R1, CCNE1 and CDKN2B were significantly increased, whereas the expression of ATM, MCM2, MRE11A and p53 was decreased in response to knockdown of ZNF403 in both Hep-2 and HEK293 cells (Figure 5c). Among those genes, the expression change of p21, MCM2, MRE11A and ATM in response to ZNF403 knockdown were further confirmed by Western blot analysis (Figure 5d). Functional annotation indicated that the gene categories particularly affected were those involved in cell cycle checkpoints. The decrease of MCM2, a component of the DNA replication licensing complex that marks DNA synthesis origins, helps us interpret the slowdown in cell-cycle S phase in response to ZNF403 knockdown. Our result also demonstrated that p21 was remarkably up-regulated both at mRNA and protein level by ZNF403 knockdown. p21/WAF1 binds directly to cyclin-CDK complexes such as Cdc2 and regulates their kinase activity by inducing cell cycle arrest[15]. The induction of p21 has been reported to be associated with G2/M arrest[16-17]. Thus, the G2/M arrest resulted from ZNF403 knockdown might be due to the up-regulation of p21. In addition, our study demonstrated a remarkable down-regulation of MRE11A/ATM by ZNF403 knockdown. MRE11A and ATM are critical components of the cell-cycle machinery for detection, signaling, and repair of DNA damage [18-19]. MRE11A facilitates the activation of ATM after DNA damage. It is likely that ZNF043 may interfere with the regulation of MRE11A/ATM pathway, thus the deletion of ZNF403 cause disturbance at G2/M checkpoint. Besides, down-regulation of endogenous ZNF403 also result in significant changes of CDK5R1 (p35), SKP2 and CDKN2B in Hep-2 and HEK293 cells. These genes are all closely linked to cell-cycle control. Further determining their relationships with ZNF403 will provide insights into understanding its role in cell-cycle regulation.

3 Discussion

In this report, we first examined the expression pattern of ZNF403 and its alternative splicing isoform LCRG1 in various human tumor cell lines. The results demonstrated that the expression level of ZNF403 is remarkably higher (>10 fold) than LCRG1, and ZNF403 is the major transcript from ZNF403 gene. Furthermore, function analysis revealed that knockdown of ZNF403 inhibited cell growth of Hep-2 both *in vitro* and *in vivo*. In contrast, previous study has shown that over expression of LCRG1 leads to suppression of Hep-2 cell. Thus, interestingly, ZNF403 and LCRG1, two isoforms from a single gene, displayed opposite functions in cell proliferation. It is widely known that alternative splicing plays a major role in the control of cell growth by dictating of the production of different isoforms with different biochemical properties and thus distinct functions, even with opposite functions[20-21]. Alternative splicing resulting in opposite functions has been documented for many genes, including Bcl-x, p53, APAF-1, Mcl-1 caspases (3～5) and so on[22-23]. Many known proto-oncogenes and tumor-suppressor genes are regulated by alternative splicing and thereby activated post-transcriptionally to allow cells to escape normal controls on cell growth and proliferation. Our observations provide insights into the effect of ZNF403 and LCRG1 in cell growth from the point of alternative splicing. They might contribute together to regulate cell proliferation in normal cells when their expression level is kept in proportion. Further study is required to elucidate their relationship in detail.

Ggnbp2, the mouse homolog of ZNF403, can be induced by 2, 3, 7, 8-Tetrachlorodibenzo-p-dioxin (TCDD, dioxin) mediated by the Aryl hydrocarbon receptor (AhR) pathway and played a pivotal role in regulation of meiotic events during spermatogenesis[12]. Our results of knockdown ZNF403 delayed mitosis is consistent with the impact of ZNF403 in mitosis in mouse studies and further provide strong evidences that ZNF403 might promote mitosis by controlling G2/M cell-cycle checkpoint. TCDD, the most potent carcinogen ever evaluated, is extremely stable and widely distributed environmental pollutant[24]. It acts as a "tumor promoter" in multiple sites and at multiple

stages during carcinogenesis [25]. TCDD exposure is associated with an increase in tumor incidence and is believed to mediate toxicity mainly through binding to AhR [26], though their mechanism is not well defined. Based on the induction of ZNF403 by TCDD through AHR and the role of ZNF403 in tumor growth, it is possible that ZNF403 might be an essential mediator to promote carcinogenesis through regulating cell-cycle progression in TCDD/AHR pathway. Thus, further clarify the mechanism of the TCDD/AHR/ ZNF403 signaling will help us to understand the role of ZNF403 in environmental carcinogenesis. Since our results showed that knocking down ZNF403 not only inhibit cell proliferation in Hep-2 *in vitro*, but also suppress the tumor Xenograft growth in nude mice, it is implied that down regulation of ZNF403 may provide a new strategy for therapeutic use in tumor cells.

Additionally, we performed cell-cycle PCR array to investigate the molecular mechanism under the inhibition of DNA synthesis and delay of mitosis caused by ZNF403 knockdown. The results revealed that a number of key cell-cycle genes were altered in response to reduction of endogenous ZNF403, such as ATM, p21, MCM2, p53, skp2, CDK5R1 (p35) and CDKN2B. As a nuclear protein, ZNF403 might mediate these target genes through transcription regulation directly or indirectly. ZNF403 may bind to their promoters and act as a transcription factor for these genes. Further examining the mechanism of ZNF403's regulation on the expression of these cell cycle related genes will help us understand the role of ZNF403 in cell cycle regulation.

These gene expression changes may be responsible for the observed effect of repression of DNA replication and G2/M cell-cycle arrest. It is known that p21 and p53 both suppress tumors by promoting cell cycle arrest in response to various stimuli. Studies also demonstrated that p21 can act as a master regulator of multiple tumor suppressor pathways for promoting anti-proliferative activities in a p53-independent mechanism [15]. In our study, ZNF403 knockdown resulted in up-regulation of p21 and down-regulation of p53. Notably, the elevation of p21 was further confirmed at protein level. It is possible that p21 may exert a more prominent role than p53 in ZNF403-mediated cell cycle regulation. Our study also showed a 2-fold decrease of MCM2, a component of the DNA replication licensing complex that marks DNA replication origins, as a consequence of ZNF403 knockdown. MCM2 was reported to be only expressed in proliferating cells and was considered a marker for colorectal cancer [27–28]. This finding is consistent with the growth inhibition from ZNF403 knockdown as measured by MTT and flow cytometric assays and further confirmed the important role of ZNF403 on growth with involvement of MCM2.

In addition, our study demonstrated a remarkable down-regulation of MRE11A/ATM by ZNF403 knockdown. MRE11A and ATM are critical components of the cell-cycle machinery for detection, signaling, and repair of DNA damage [18–19]. MRE11A facilitates the activation of ATM after DNA damage. ATM, which is recruited and activated by DNA double-strand breaks, phosphorylates a number of key cell-cycle proteins including p53, CHK2, RAD17, BRCA1 and initiates cell cycle arrest at checkpoints[18]. The phosphorylation of p53 by ATM can result in the accumulation and activation of p53 in the nucleus [29]. Based on the known signal pathway and that all of these 3 genes were down-regulated by ZNF403 knockdown, it is suggested that ZNF043 may be an upstream regulator of the MRE11A/ATM/p53 pathway. Moreover, down-regulation of endogenous ZNF403 also leads to significant changes of CDK5R1 (p35), SKP2 and CDKN2B in Hep-2 and HEK293 cells. These genes are all closely linked to cell-cycle control. CDK5R1 (p35), a specific activator of the serine/threonine kinase CDK5, plays crucial roles in CNS development and maintenance [30]. Skp2 is the F-box component of an E3 ubiquitin ligase complex that targets p27 (Kip1) and cyclin E1 to the proteasome. It is reported that targeted proteasomal degradation mediated by E3 ubiquitin ligases controls cell cycle progression, and alterations in their activities likely contribute to malignant cell proliferation [31]. CDKN2B, also known as p15Ink4b protein, forms a complex with CDK4 or CDK6, and prevents the activation of the CDK kinases by cyclin D, thus acts as a cell growth regulator that inhibits cell cycle G1 progression [32]. It is possible that the up-regulation of CDKN2B might be an effector of ZNF403-mediated reduction of DNA synthesis. Further investigation will be conducted on the mechanism of ZNF403's

regulation on cell cycle progression and the relationship between ZNF403 and these genes.

In conclusion, our study uncovered that the expression pattern of ZNF403 and LCRG1 and suggest a role of ZNF403 as an oncogene associated with cell-cycle control as well as potential use of down-regulation of ZNF403 for tumor suppression in cancer therapy.

References

[1] Rudolph E, Dyckhoff G, Becher H, *et al*. Effects of tumour stage, comorbidity and therapy on survival of laryngeal cancer patients: a systematic review and a meta-analysis. Eur Arch Otorhinolaryngol, 2011, **268** (2): 165-179(DOI:10.1007/s00405-010-1395-8)

[2] Islami F, Tramacere I, Rota M, *et al*. Alcohol drinking and laryngeal cancer: overall and dose-risk relation——a systematic review and meta-analysis. Oral Oncol, 2010, **46** (11): 802-810 (DOI:S1368-8375 (10)00231-9 [pii]10.1016/j.oraloncology. 2010.07.015)

[3] Abbasi R, Ramroth H, Becher H, *et al*. Laryngeal cancer risk associated with smoking and alcohol consumption is modified by genetic polymorphisms in ERCC5, ERCC6 and RAD23B but not by polymorphisms in five other nucleotide excision repair genes. Int J Cancer, 2009, **125** (6): 1431-1439(DOI:10.1002/ijc.24442)

[4] Sokic S I, Adanja B J, Marinkovic J P, *et al*. Risk factors for laryngeal cancer. Eur J Epidemiol, 1995, **11** (4): 431-433

[5] Makitie A A, Monni O. Molecular profiling of laryngeal cancer. Expert Rev Anticancer Ther, 2009, **9** (9): 1251-1260(DOI:10.1586/ era.09.102)

[6] Loyo M, Pai S I. The molecular genetics of laryngeal cancer. Otolaryngol Clin North Am, 2008, **41** (4): 657-672 (DOI:S0030-6665(08)00030-3[pii]10.1016/j.otc.2008.01.019)

[7] Glynn R W, Miller N, Kerin M J. 17q12-21 - the pursuit of targeted therapy in breast cancer. Cancer Treat Rev, **36** (3): 224-229 (DOI: S0305-7372(09)00189-3[pii]10.1016/j.ctrv.2009.12.007)

[8] Levin A M, Machiela M J, Zuhlke K A, *et al*. Chromosome 17q12 variants contribute to risk of early-onset prostate cancer. Cancer Res, 2008, **68** (16): 6492-6495(DOI:68/16/6492[pii]10.1158/0008-5472.CAN-08-0348)

[9] Li Y, Chen Z. Molecular cloning and characterization of LCRG1 a novel gene localized to the tumor suppressor locus D17S800-D17S930. Cancer Lett, 2004, **209** (1): 75-85(DOI:10.1016/j.canlet. 2003.11.034 S0304383503008309[pii])

[10] Li Y J, Xie H L, Chen Z C. Cloning and expression analysis of a laryngeal carcinoma related gene, LCRG1. Acta Biochem Biophys Sin, 2001, **33** (3): 315-319

[11] Zhang J, Wang Y, Zhou Y, *et al*. Yeast two-hybrid screens imply that GGNBP1, GGNBP2 and OAZ3 are potential interaction partners of testicular germ cell-specific protein GGN1. FEBS Lett, 2005, **579** (2): 559-566(DOI:S0014-5793(04)01560-1[pii]10.1016/ j.febslet.2004.10.112)

[12] Ohbayashi T, Oikawa K, Iwata R, *et al*. Dioxin induces a novel nuclear factor, DIF-3, that is implicated in spermatogenesis. FEBS Lett, 2001, **508** (3): 341-344(DOI:S0014-5793(01)03039-3[pii])

[13] Guan R, Wen X Y, Wu J, *et al*. Knockdown of ZNF403 inhibits cell proliferation and induces G2/M arrest by modulating cell-cycle mediators. Mol Cell Biochem, 2012, **365** (1-2): 211-222

[14] Puntervoll P, Linding R, Gemund C, *et al*. ELM server: A new resource for investigating short functional sites in modular eukaryotic proteins. Nucleic Acids Res, 2003, **31** (13): 3625-3630

[15] Abbas T, Dutta A. p21 in cancer: intricate networks and multiple activities. Nat Rev Cancer, 2009, **9** (6): 400-414(DOI:nrc2657[pii] 10.1038/nrc2657)

[16] Ando T, Kawabe T, Ohara H, *et al*. Involvement of the interaction between p21 and proliferating cell nuclear antigen for the maintenance of G2/M arrest after DNA damage. J Biol Chem, 2001, **276** (46): 42971-42977 (DOI:10.1074/jbc.M106460200 M106460200[pii])

[17] Choi Y H, Zhang L, Lee W H, *et al*. Genistein-induced G2/M arrest is associated with the inhibition of cyclin B1 and the induction of p21 in human breast carcinoma cells. Int J Oncol, 1998, **13** (2): 391-396

[18] Carson C T, Schwartz R A, Stracker T H, *et al*. The Mre11 complex is required for ATM activation and the G2/M checkpoint. EMBO J, 2003, **22** (24): 6610-6620(DOI:10.1093/emboj/cdg630)

[19] Lee J H, Paull T T. Direct activation of the ATM protein kinase by the Mre11/Rad50/Nbs1 complex. Science, 2004, **304** (5667): 93-96 (DOI:10.1126/science.1091496 304/5667/93[pii])

[20] David C J, Manley J L. Alternative pre-mRNA splicing regulation in cancer: pathways and programs unhinged. Genes Dev, 2010, **24** (21): 2343-2364

[21] Venables J P, Klinck R, Koh C, *et al*. Cancer-associated regulation of alternative splicing. Nat Struct Mol Biol, 2009, **16** (6): 670-676 (DOI:nsmb.1608[pii]10.1038/nsmb.1608)

[22] Pecci A, Viegas L R, Baranao J L, *et al*. Promoter choice influences alternative splicing and determines the balance of isoforms expressed from the mouse bcl-X gene. J Biol Chem, 2001, **276** (24): 21062-21069 (DOI:10.1074/jbc.M008665200

M008665200[pii])

[23] Ghosh A, Stewart D, Matlashewski G. Regulation of human p53 activity and cell localization by alternative splicing. Mol Cell Biol, 2004, **24** (18): 7987−7997 (DOI:10.1128/MCB.24.18.7987-7997.2004 24/18/7987[pii])

[24] Ray S, Swanson H I. Activation of the aryl hydrocarbon receptor by TCDD inhibits senescence: a tumor promoting event?. Biochem Pharmacol, 2009, **77** (4): 681−688 (DOI:S0006-2952 (08)00856-3 [pii]10.1016/j.bcp.2008.11.022)

[25] Mimura J, Fujii-Kuriyama Y. Functional role of AhR in the expression of toxic effects by TCDD. Biochim Biophys Acta, 2003, **1619**(3): 263−268

[26] Bock K W, Kohle C. Ah receptor- and TCDD-mediated liver tumor promotion: clonal selection and expansion of cells evading growth arrest and apoptosis. Biochem Pharmacol, 2005, **69** (10):1403−1408 (DOI:S0006-2952 (05)00090-0 [pii]10.1016/j.bcp.2005.02.004)

[27] Cho J H, Kim H B, Kim H S, *et al*. Identification and characterization of a rice MCM2 homologue required for DNA replication. BMB Rep, 2008, **41** (8): 581−586

[28] Hanna-Morris A, Badvie S, Cohen P, *et al*. Minichromosome maintenance protein 2 (MCM2) is a stronger discriminator of increased proliferation in mucosa adjacent to colorectal cancer than Ki-67. J Clin Pathol, 2009, **62** (4): 325−330 (DOI:jcp.2007.054643 [pii]10.1136/jcp.2007.054643)

[29] Cheng Q, Chen J. Mechanism of p53 stabilization by ATM after DNA damage. Cell Cycle, 2010, **9** (3): 472-478(DOI:10556[pii])

[30] Moncini S, Salvi A, Zuccotti P, *et al*. The role of miR-103 and miR-107 in regulation of CDK5R1 expression and in cellular migration. PLoS One, 2011, **6** (5): e20038 (DOI:10.1371/journal.pone.0020038 PONE-D-10-05556[pii])

[31] Hu R, Aplin A E. Skp2 regulates G2/M progression in a p53-dependent manner. Mol Biol Cell, 2008, **19** (11): 4602−4610 (DOI:E07-11-1137[pii]10.1091/mbc.E07-11-1137)

[32] Hannon G J, Beach D. p15INK4B is a potential effector of TGF-beta-induced cell cycle arrest. Nature, 1994, **371** (6494): 257−261(DOI:10.1038/371257a0)

ZNF403，一个新的细胞周期调节因子的功能研究 *

关　瑞[1,2,3]　侯德富[1,2]　饶　翔[2]　关勇军[2]
欧阳咏梅[2]　余艳辉[2]　Jim HU[3]　陈主初[1,2]**
([1]中南大学湘雅医院卫生部肿瘤蛋白质组学重点实验室，长沙 410008；[2]中南大学肿瘤研究所，长沙 410008；
[3] *Physiology and Experimental Medicine Program, Hospital for Sick Children, Toronto, Ontario* M5G1X8, Canada)

摘要　ZNF403 和 LCRG1 是人类基因 ZNF403 的 2 个不同转录剪切本．以往的研究表明 LCRG1 在喉癌细胞株 Hep-2 中具有抑瘤特性．本研究旨在探明 ZNF403 和 LCRG1 不同剪切本之间的关系以及在肿瘤细胞中对 ZNF403 的功能进行研究．首先，采用实时荧光定量 PCR 对这 2 个转录本的相对表达水平进行分析，结果表明，ZNF403 表达水平在不同细胞株中明显高于 LCRG1(>10 倍)，为该基因的主要转录表达产物．随后分别采用 MTT 细胞生长分析法和裸鼠体内成瘤实验在体外和体内对 ZNF403 的功能进行分析，结果显示 ZNF403 的基因沉默可以同时在体内和体外抑制喉癌细胞 Hep-2 细胞的生长．为了探明其作用机制，本研究还采用细胞信息学、流式细胞周期分析术和高通量 PCR 点阵分析方法进一步分析，结果表明，ZNF403 的基因沉默可显著抑制细胞 DNA 的复制并延缓细胞周期进入到有丝分裂期．同时发现 ZNF403 可调节一系列的细胞周期调节蛋白如 MCM2、p21、ATM、MRE11A 等．综上研究提示 ZNF403 为一新的细胞周期调节因子，其功能的缺失与肿瘤发生发展密切相关．

关键词　ZNF403，LCRG1，选择性剪切，细胞周期，AhR
学科分类号　Q71，Q354　　**DOI**: 10.3724/SP.J.1206.2012.00119

* 国家留学基金委高水平项目资助, 加拿大卫生研究院(CIHR)研究基金资助项目, 国家重点基础研究发展计划项目 (2011CB9107040)和国家自然科学基金(30973289, 81272971)资助项目.
** 通讯联系人.
Tel: 0731-84327608, E-mail: tcbl@xysm.net
收稿日期：2012-05-15，接受日期：2012-09-29